Received: 17 June 2022 | Revised: 7 September 2022 | Accepted: 2 October 2022

DOI: 10.1002/pc.27107

RESEARCH ARTICLE

spe INSPIRING PLASTICS PROFESSIONALS Polymer COMPOSITES WILEY

Spray binder for automated preforming: Spray process and preform properties

Hendrik Möllers[1] | **Carsten Schmidt**[2] | **Dieter Meiners**[3]

[1]Institute of Polymer Materials and Plastics Engineering, Clausthal University of Technology, Stade, Germany

[2]Institute of Production Engineering and Machine Tools, Leibniz Universität Hannover, Stade, Germany

[3]Institute of Polymer Materials and Plastics Engineering, Clausthal University of Technology, Clausthal-Zellerfeld, Germany

Correspondence
Hendrik Möllers, Institute of Polymer Materials and Plastics Engineering, Clausthal University of Technology, Ottenbecker Damm 12, Stade, Germany.
Email: hendrik.moellers@tu-clausthal.de

Funding information
European Regional Development Fund

Abstract

A closer look was taken at a spray binder and the properties of the preforms made with said binder and non-crimp carbon fiber textiles. First the spray process was analyzed, then T-peel and three point flexural tests were carried out to compare the spray binder to other binder systems. While the spray binder showed higher peel strength than most binders found in literature, the measured flexural strength was lower than the values found for powder.

KEYWORDS

composites, mechanical testing, processing, thermosets

1 | INTRODUCTION

Fiber-reinforced plastics offer unique advantages for lightweight applications including high strength, stiffness and corrosion resistance.[1] Different production techniques for fiber reinforced plastics have been developed in the past including prepreg and liquid composite molding (LCM) processes.[2] An important step in the LCM-process chain is the manufacturing of a preform, which is later infused with a resin to obtain the final part.[3,4] To ensure sufficient stability of the preforms different technologies are available. Layers of semi-finished products such as woven or non-crimped fabrics can be stacked and fixed by sewing, stitching or the application of so called binders or tackifiers in-between the textile layers. Direct preforming technologies like dry fiber placement or fiber injection molding allow the manufacturing of preforms without semi-finished products.[4–9] This paper focuses on the use of binders and preforms made from non-crimped fabrics. Commercial binder systems are available in different forms, common ones include powders,[10–12] veils,[13,14] preimpregnated fibers,[14–16] binders dissolved in solvent[14,17] or hotmelts.[14,18–22]

Different polymers can be used as binders. Depending on their interaction with the matrix material, there are two different binder classes: reactive and non-reactive binders. Reactive binders take part in the curing reaction of resin and hardener whereas non-reactive binders remain in the matrix as foreign matter.[23] Reactive binders are usually thermoset polymers, while non-reactive binders are often thermoplastics. However, the specific interaction between binder and resin may vary depending on the type of resin used for infusion or injection. Many different polymers are used as binders including epoxies, phenoxies, copolyamide and polyolefins.[18,23,24]

Research in past years has shown the importance of understanding the interactions between binders and resin as they influence all following steps of the LCM-process chain. Binders can increase the viscosity of the resin and influence its curing time affecting the infusion step.[10,11,24,25] They also affect the permeability positively or negatively depending on binder type, application and measurement technique, further affecting the preform infusion.[24,26–30] The impact of binders on the mechanical properties of the final part was also studied over the past two decades. For epoxy-based binders, Tanoglu et al. found a negative influence on the fracture toughness compared to parts manufactured without binder while Hillermeier reports a positive influence.[17,31] Brody and Gillespie found a negative influence of the binder on void content, interlaminar shear strength and fracture toughness.[23] More recent work in which different binder chemistries were studied has shown the importance of carefully choosing a suited binder depending on the matrix system. Depending on the chosen binder system and resin the mechanical properties can be affected both ways or remain unchanged.[5,12,22] Lastly, the influence of binder on the preform properties was subject of multiple publications. T-peel test and flexural test were carried out to determine the fixation of the layers to each other and the ability of the binder to hold the preform in its given 3-D shape.[10,11,24,31–33]

The presented research on preform properties is mainly focused on the use of binder powders or veils, which are solid at room temperature. They are melted after application to bond the textile layers together. In efforts to automate preform manufacturing, spray processes are often used instead of classic powder application or veils.[3,19,20,34] When spraying melted binder powder[35,36] or hotmelts, the binder loses heat and the ability to bond the textile layers together rapidly.[37,38] Consequently, the binder often has to be reheated after its application by infrared radiators, lasers, hot gas or intrinsic fiber heating.[15,20] Spray binders with properties similar to pressure-sensitive adhesives do not have this downside. They are highly viscous at room temperature and still offer enough tackiness to bond the textile layers together. Since no research on the preform properties manufactured with this type of binder is known to the authors, this paper focuses on determining if spray binder offers properties similar to preforms made with powders or veils. First, the materials and the spray process were characterized to get a better understanding of factors affecting swirl spray deposition of spray binders. Then T-peel and three-point flexural tests were carried out with preforms made with spray binder and three different types of fiber orientations. The results were then compared to values measured for powder binders and veils from literature.

2 | EXPERIMENTAL

2.1 | Materials

The spray binder used in this publication was the epoxy based CeTePox AM1010 made by CTP Advanced Materials. At room temperature, the binder is liquid, highly viscous and offers sufficient tackiness to bond textile layers together. Two different carbon fiber non-crimped fabrics were used. An unidirectional textile by Kümpers with a grammage of 620 g/m^2 fixed by a polyester sewing yarn and a biaxial textile by Kümpers with a grammage of 600 g/m^2 also fixed by a polyester sewing yarn.

2.2 | Material characterization

The viscosity of the binder was measured using an TA Instruments Ares G2 oscillation rheometer. The binder was placed between two parallel aluminum plates with a diameter of 40 mm preheated to the starting temperature of 55°C. The gap between the plates was then set to 1 mm. As the binder viscosity has decreased significantly at 55°C the binder fills the gap. Excess binder flows out of the gap and is removed prior to the start of the measurement. The binder has to cover both plates completely. The full test setup is shown in Figure 1. To measure the influence of temperature on viscosity, the frequency was set to 1 Hz. Starting temperature was 55°C, heating up to 130°C with a heating rate of 1 K/min. To analyze the influence of shear rate measurements at 55, 80, 95, and 110°C were made. The shear rate range used was 0.01 to 100 Hz.

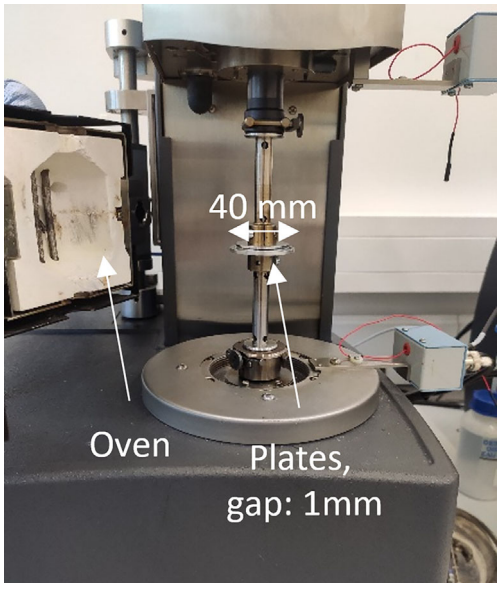

FIGURE 1 Test setup for viscosity measurements

The surface of the textiles was analyzed with a Keyence VK-X1000 3D profilometer. Surface scans were made for both textiles and an average surface profile was created perpendicular to the fiber orientation.

2.3 | Spray parameters

A swirl spray module with 12 GHS401-22 SC spray heads made by Gluematic was used to investigate the influence of material temperature and material pressure on the amount of binder sprayed. The binder is put into a glue gun (rb-TPR-250-LCD by ratiobond) and then forwarded into the spray module by compressed air (2 bar ... 6 bar). Glue gun and spray module can be heated up to 200°C. Figure 2 shows a schematic drawing of the glue gun connected to a single spray head. The full setup with all 12 spray heads is shown in Figure 3. The spray module is equipped with an additional heating unit for the compressed air (spray air) used to create the swirl. This delays the cooling of the spray binder after leaving the spray nozzle, ensuring an even binder coating on the surface of the textile. The temperature was varied between 90 and 120°C. In this window, the binder is at a suitable viscosity for spraying without the risk of altering the binder's properties (a change in material properties happens at 150°C and above). The air pressure for binder forwarding was varied between 2 bar and 6 bar. Spray air pressure was kept at 1 bar. The results were used to develop a spraying strategy for the following sample manufacturing.

2.4 | Sample manufacturing

The samples were made by the in-house developed continuous wet draping (CWD)–process, a process for automated preform manufacturing. The CWD-setup is shown in Figure 4. Further details regarding the CWD-process can be found in Denkena et al.[39]

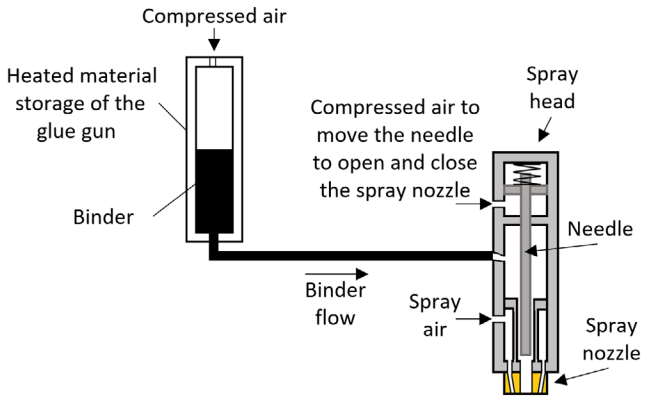

FIGURE 2 Schematic drawing of the spraying set-up

Within the process, the laying speed can reach up to 100 mm/s. This allows controlling the amount of binder sprayed on the textile independently of the spray module. The binder was sprayed on the textile at a temperature of 95°C with a material pressure of 2 bar. Different binder grammages were sprayed onto the textiles by varying the laying speed of the CWD-system. As the binder is highly viscous at room temperature but not solid, it will eventually flow out of the interlayer between the textiles. Therefore, the binder manufacturer recommends processing the preforms within 2 weeks of manufacturing. To avoid influencing the results, all samples were tested within 2 days after sample manufacturing.

After binder application, the layers were draped onto a flat surface by the shape replicating draping unit. The draping unit is path controlled and can be adjusted to the fabric thickness. As both textiles have a thickness of around 0.6 mm when infused via vacuum infusion, the gap between the plate and the draping unit was set to 0.6 mm * number of layers. A negative effect of the path controlled draping unit is the currently unknown variance of the compression pressure while following complex geometries. However, this did not affect the sample manufacturing. due to the flat surfaced used for sample preparation. With no movement of the draping unit the pressure during sample manufacturing was constant. The test results of all samples showed no indication of varying compression pressure during sample manufacturing. The absolute value of the compression pressure is unknown which has to be considered when evaluating the test results.

2.5 | T-peel test

T-peel tests were performed according to DIN EN ISO 11339[40] on a Zwick&Roell Z005. Preforms with 20, 40, and 80 g/m^2 of binder were tested. Those grammages equal roughly 2, 4, and 8 wt% of binder at a fiber volume content of 50%. To get information about the influence of layer orientations towards the test machine as well as within the lay-up, different lay-ups were investigated. Table 1 shows the tested lay-ups and binder grammages. For every combination of lay-up and binder grammage five samples were tested. The size of the samples was 250 mm × 25 mm with 50 mm of the 250 mm binderfree for clamping. A schematic drawing of the test setup can be seen in Figure 5.

2.6 | Three-point flexural test

Due to the low flexural strength and modulus measured in other publications the flexural tests were carried out

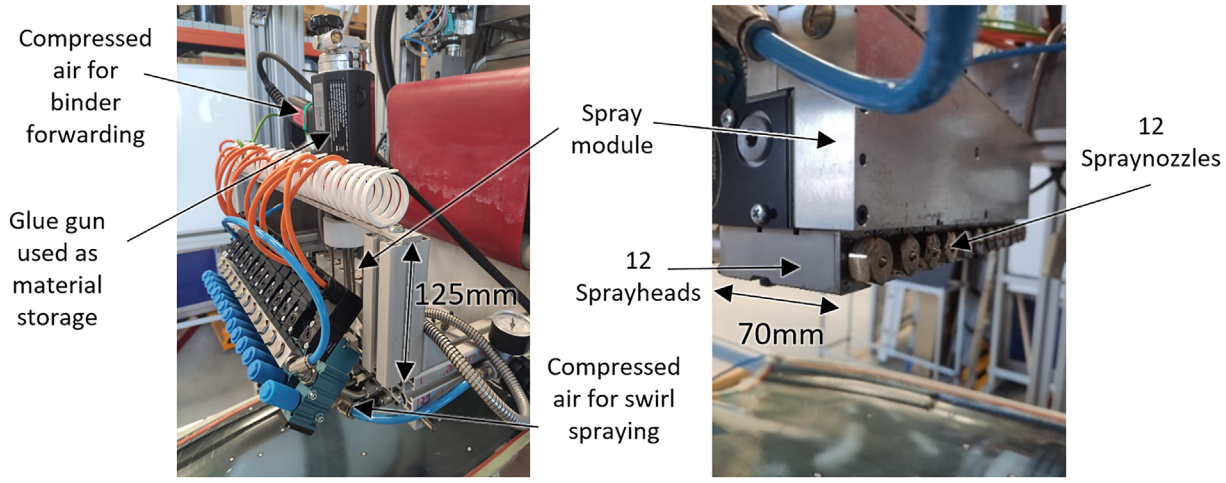

FIGURE 3 Spray setup and close-up of the spray module

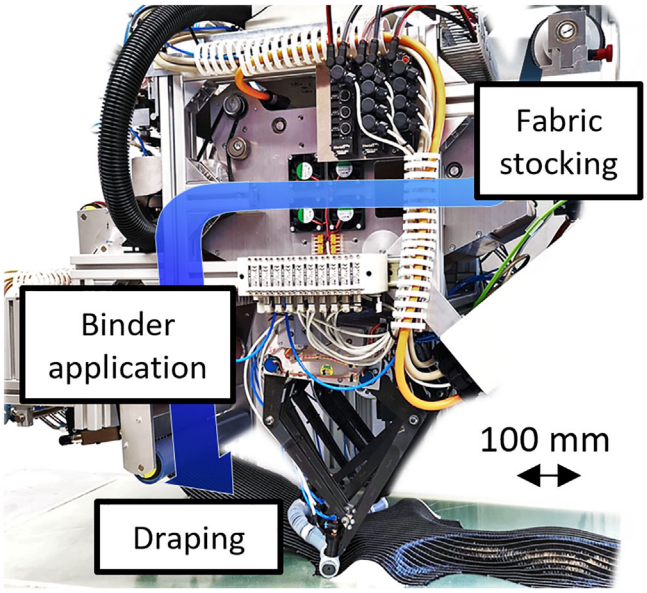

FIGURE 4 CWD-lay-up-head

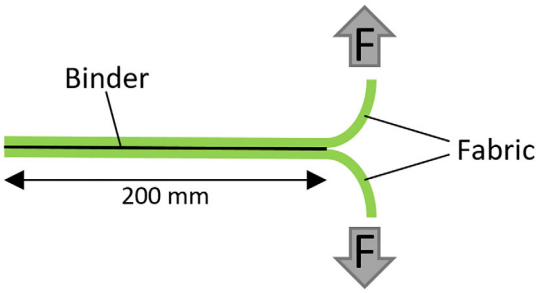

FIGURE 5 Schematic drawing T-peel test DIN EN ISO 11339

TABLE 1 Lay-ups and binder grammages for T-peel tests

Lay-up	Binder grammage
UD/UD, UD/(0°/90°), UD/±45°, (0°/90°)/(0°/90°), ±45°/(0°/90°), ±45°/±45°	20 g/m^2, 40 g/m^2, 80 g/m^2

on the TA Instruments Ares G2 oscillation rheometer. The rheometer offers the possibility of measuring small axial forces up to 20 N. Based on DIN EN ISO 14125[41] a test device was 3-D printed and mounted onto the rheometer. After aligning the test device, the motor of the rheometer is locked to avoid rotation of the test device. The resulting test setup can be seen in Figure 6. As for the T-peel test, samples with 20, 40, and 80 g/m^2 of

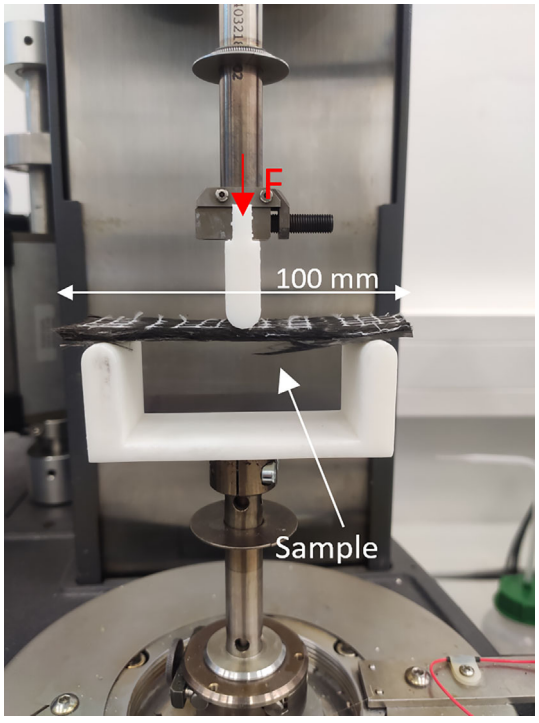

FIGURE 6 Test setup three-point flexural test

TABLE 2 Lay-ups, binder grammages and test speeds for three-point flexural tests

Lay-up	Binder grammage	Test speed
$(0°)_4$, $(0°/90°)_4$, $(\pm45°)_4$	20 g/m^2, 40 g/m^2, 80 g/m^2	4 mm/min; 60 mm/min

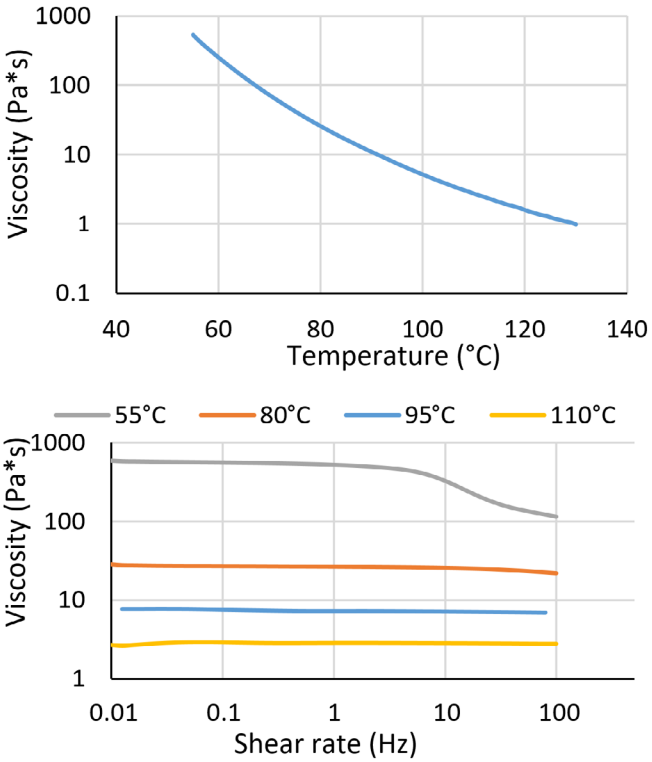

FIGURE 7 Viscosity of CeTePox AM1010 depending on temperature and shear rate

binder were made. 0°-samples were prepared from the unidirectional textile, 0°/90°- and ±45°-samples from the biaxial textile. All samples consist of four textile layers and were cut to be 100 mm long and 25 mm wide. Two test speeds were chosen: 60 mm/min as used by Dickert[24] and 4 mm/min as recommended by DIN EN ISO 14125[41] for fiber-reinforced plastics of the sample's thickness. Preliminary testing has shown that at 60 mm/min the measured flexural strength and modulus increase up to 50% for the unidirectional samples compared to 4 mm/min. As the binder is not solid at room temperature, a high influence of testing speed is expected. Using two different testing speeds allows to compare the results to Dickert as well as investigating the influence of test speed on the highly viscous binder. Since the samples did not fail but were only deformed before falling of the test device, all tests were stopped after 20 mm of travel. Table 2 shows the tested combinations. Due to the high number of possible lay-ups with four layers only samples with four identical layers were prepared. For every combination of lay-up, binder grammage and test speed five samples were tested.

3 | RESULTS AND DISCUSSION

3.1 | Binder viscosity and sprayability

The results of the viscosity measurements can be found in Figure 7. With increasing temperature, the viscosity drops quickly reaching 1 Pa*s at 130°C. The influence of the shear rate varies for different temperatures. While significant shear thinning can be observed in the 55°C–curve, the viscosity shows almost no dependency on the shear rate for higher temperatures. According to Hepperle,[42] shear rates during pipe flows (which is most of the material forwarding) reach around 10 Hz. At the temperatures used during sample manufacturing, the spray binder can therefore be described as a Newtonian fluid with a viscosity independent of shear rate.[43,44]

The influence of pressure and temperature on the amount of binder sprayed is displayed in Figure 8.

Binder flow rate increases with both pressure and temperature rising. While binder flow increases linearly with rising pressure, it grows exponentially with rising temperature. This is consistent with trends indicated by the Hagen–Poiseuille equation given in Equation (1). V/t is volume flow, Δp pressure difference between inlet and outlet, R pipe diameter, η viscosity (which depends on the temperature as shown previously) and l the length of the pipe.

$$\frac{V}{t} = \frac{\pi \Delta p R^4}{8 \eta l}. \quad (1)$$

Neglecting the spray module is not a single straight pipe, the equation shows both pressure and temperature influence volume flow and therefore mass flow. Increasing the pressure results in a linear increase of the volume flow. Since the viscosity drops exponentially with increasing temperature the flow should rise exponentially with increasing temperature. This is the case for the examined binder system.

At first glance, the temperature appears suitable to regulate binder flow as a rather small temperature range covers a wide range of mass flows. The possible mass flow variation with a change in pressure is much smaller. However, to fully evaluate the spray parameters, the resulting spray pattern has to be considered, as well. Figure 9 shows the different spray patterns of a single nozzle for different temperatures, a pressure of 4 bar and

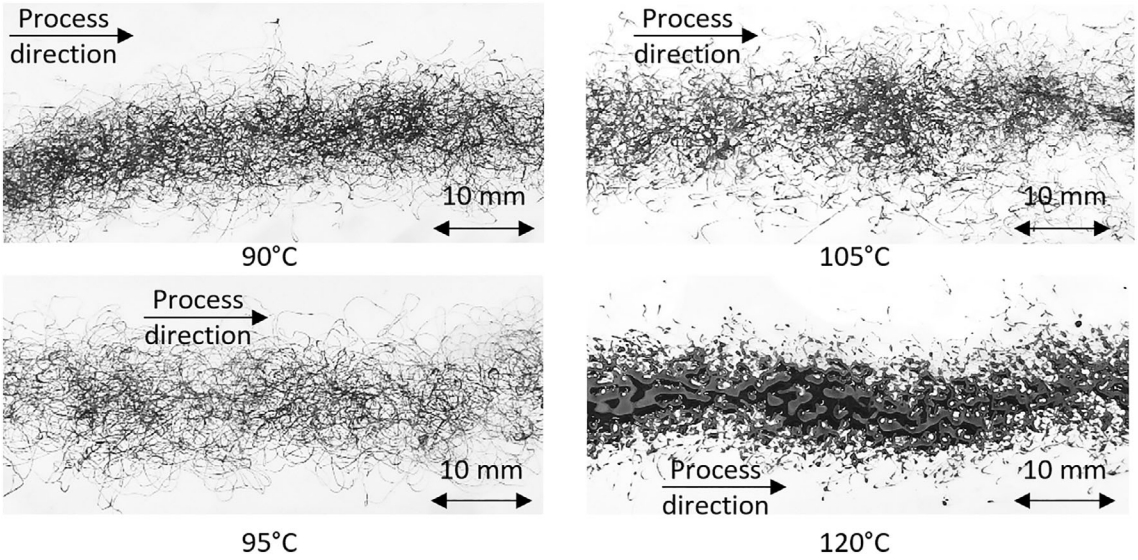

FIGURE 8 Spray pattern for different temperatures for a single nozzle spray

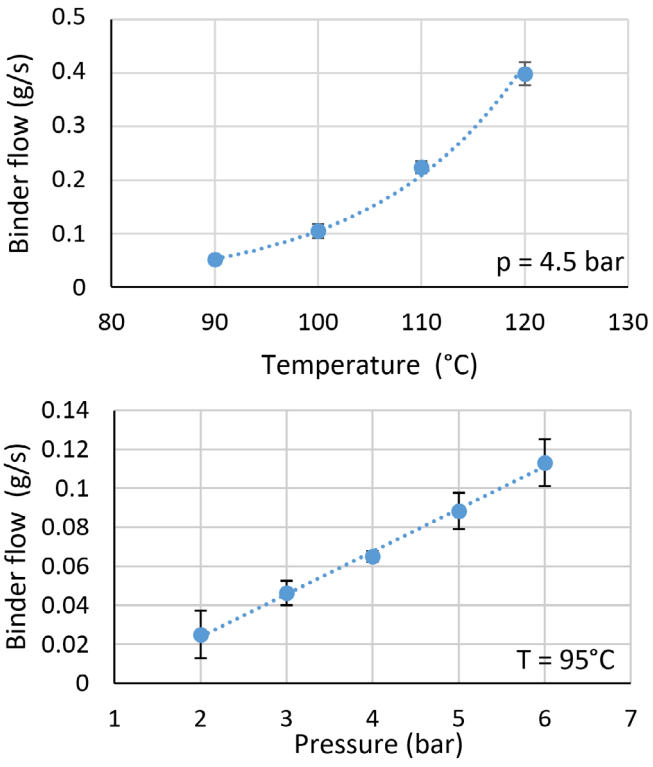

FIGURE 9 Influence of pressure and temperature on binder flow rate

a layup speed of 22 mm/s. At 85°C the binder forms knots after exiting the nozzle and an even swirl application on the textile is not possible. At 105°C and above, the swirl fiber starts breaking and forming drops, leading to an uneven spray pattern. This observation is consistent with the data sheet of CeTePox AM1010[45] which recommends temperatures between 90 and 95°C for a uniform swirl spray application and observations of Marla et al.[46]

A possible explanation for the knots is given in Formoso et al. [45]. It was shown that increasing the ratio between spray airflow and material flow increases the risk of the swirl making contact with itself and forming knots. This is the case when binder flow is lowered due to lower temperature. As a result, the spray air pressure should be adjusted when lowering the temperature. For higher temperatures, the following assumption is made: The intermolecular forces are weakened with increasing temperatures thus making it easier to break apart the swirl by airflow and supporting the development of spray mist instead of a spray swirl.

3.2 | Textile surface

The results of the surface analysis of both textiles can be seen in Figure 10. The unidirectional textile has wider tows and a higher profile. The tows of the unidirectional textile are around 4 mm wide while the biaxial ones are around 2 mm wide. A comparison of the average surface profile of both textiles is displayed in Figure 11. The yellow line shows the average surface profile of the unidirectional textile, the average surface of the biaxial textile is shown in blue. For the unidirectional textile, tows can easily be identified. Whereas, the surface profile of the biaxial textile appears to be almost flat. The tows of the unidirectional textile are also roughly twice as wide as the ones of the biaxial textile. It is assumed that the rougher profile of the unidirectional textile offers less bonding area for the binder since binder applied in-between the tows most

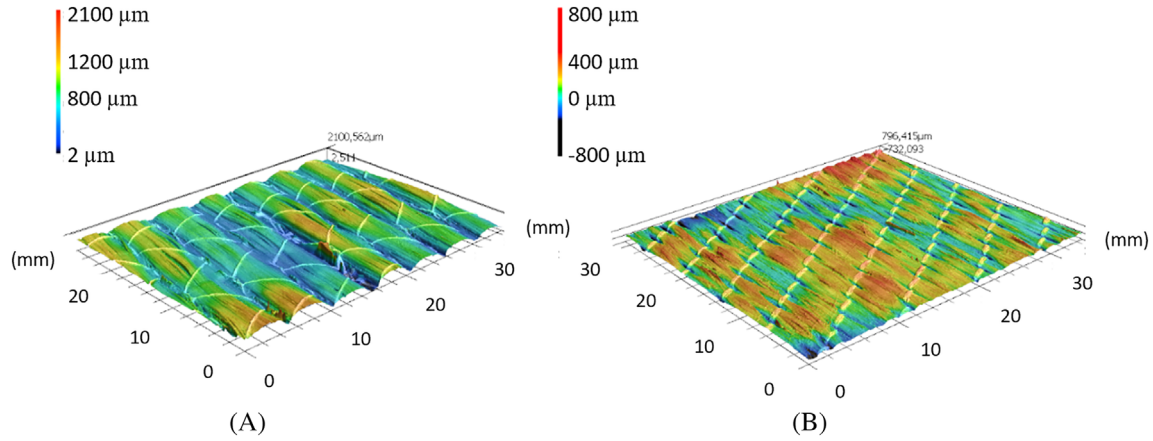

FIGURE 10 Surface scan of (A) unidirectional textile and (B) biaxial textile

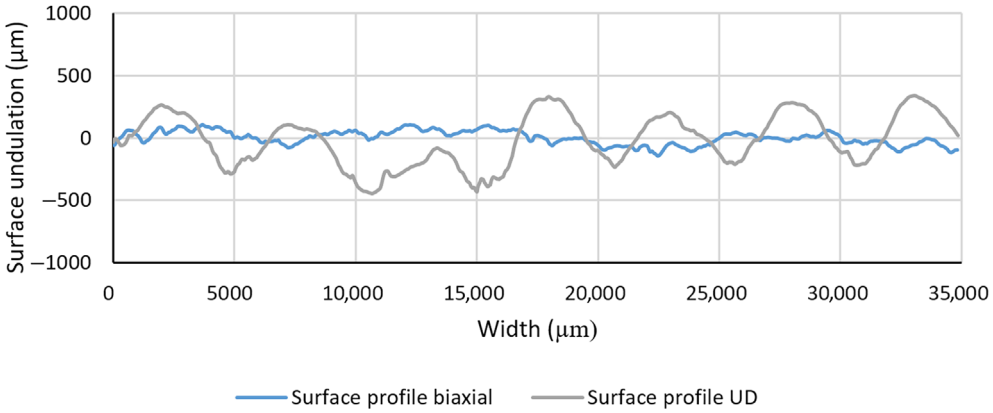

FIGURE 11 Average surface profile perpendicular to the fiber direction of the unidirectional (yellow) and biaxial (blue) textile

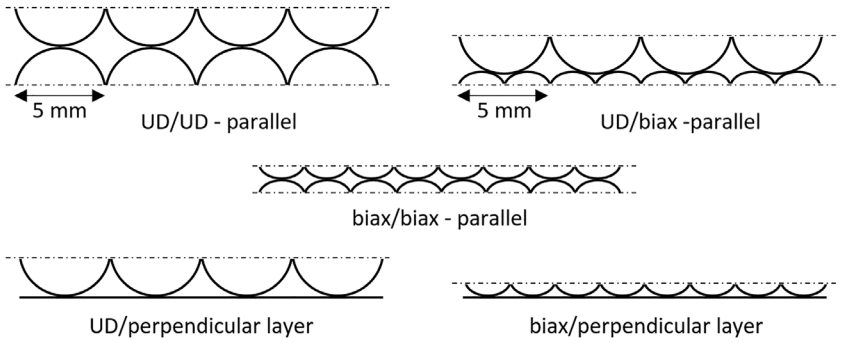

FIGURE 12 2-D schematic comparison of the contact area of the textiles for different orientations

likely does not affect the bonding between two textile layers. This effect should be especially relevant for the measurement of peel strength. If the assumption made here is true, higher peel strengths for samples made from the biaxial textile are expected. Figure 12 shows a 2-D schematic overview over the different possible combinations of surface contacts with the textiles used in this paper. It is important to note that the tows are not solid and can deform under pressure. With increasing pressure, the contact area between the layers is expected to increase thus increasing the peel strength. At higher compression pressures the likelihood of nesting between equally oriented textiles also increases. This can lead to a larger contact area. However, varying compaction pressure was not investigated within this study.

3.3 | T-peel test

Figure 13 shows the results of the T-peel test. At the lowest tested binder grammage, samples made from the unidirectional textile show lower peel forces than lay-ups

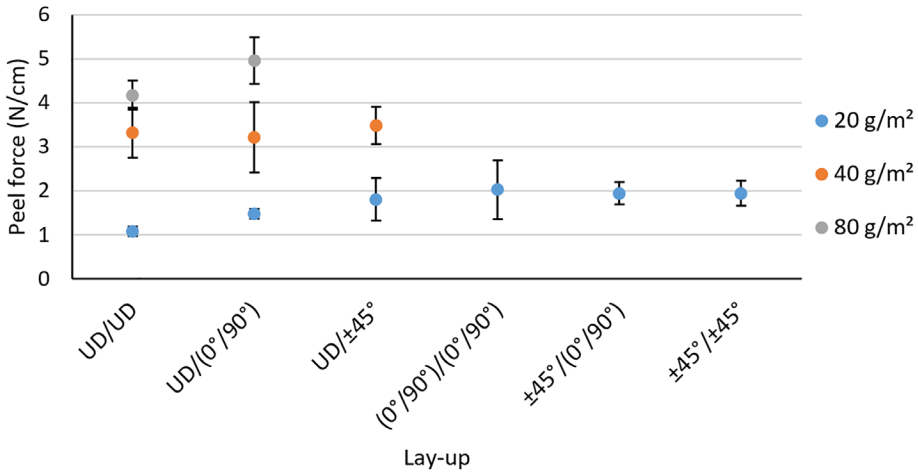

FIGURE 13 Results of T-peel test using different amounts of binder and textile orientations

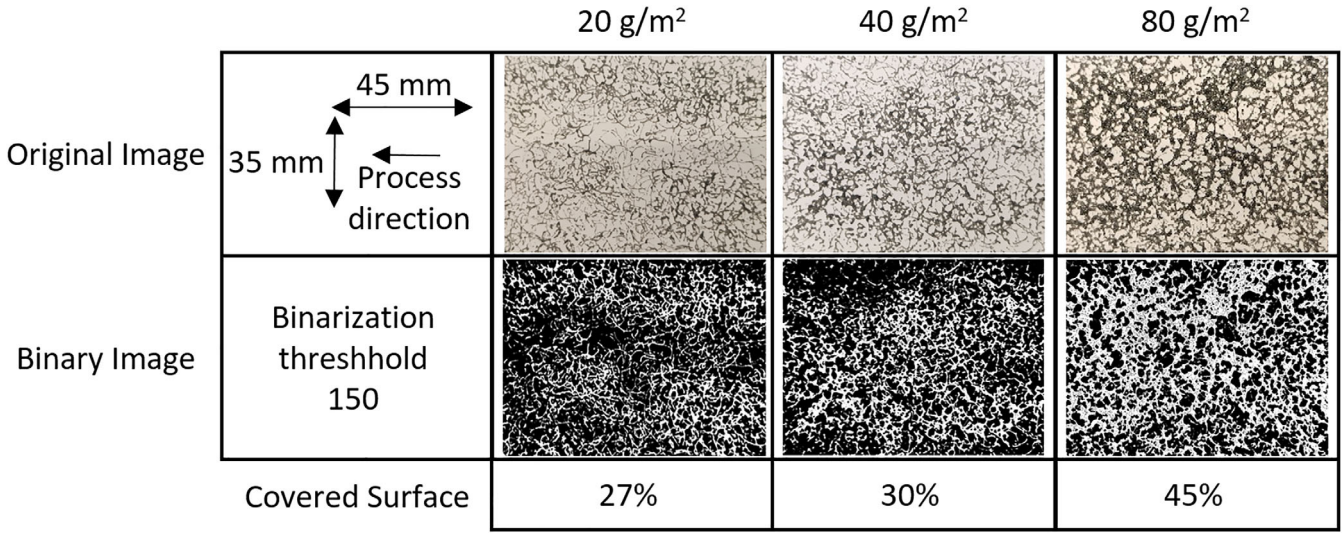

FIGURE 14 Percentage of covered surface at different binder grammages

involving the biaxial textile. Between the different fiber orientations of the biaxial textile, no difference in peel strength could be found. A possible explanation for this observation, the smaller tows within the biaxial textile, was already presented in Section 3.2. The smaller tows and lower average surface profile result in a higher contact area between the textile layers. For higher binder amounts the peel force increases. A comparison between different textiles is not possible since the knitting yarn in the biaxial textile failed before the binder in most cases of higher binder grammage. For the unidirectional textile, the peel force seems to run towards an upper limit with increasing binder grammage, whereas for the lay-up involving both textiles the peel force seems to increase linearly. Dickert[24] and Tanoglu[32] found a linear increase of peel strength for increasing binder amounts as long as there is open space on the textile surface. Increasing the binder amount when the surface is already completely covered does not increase the peel strength further (see also Reference[11]). Since the contact area of the biaxial textile is higher (see Section 3.2), there is more surface area for binder which might result in higher possible peel forces. A clear influence of the layer orientation within the lay-up is not visible. The results show that the measured peel forces depend not only on the binder system but also on the textile. To get more information on the surface covered by binder, binder was sprayed on paper at the three different lay-up speeds used for sample manufacturing. Afterwards pictures of the spray picture were taken and the surface covered by binder was measured using image binarization in Matlab. The results are displayed in Figure 14. They are not fully accurate as the color of the binder varies making it difficult to find an appropriate binarization threshold. However, the images still show an increase in covered surface area with increasing binder grammage. Moreover, there is still open space available at 80 g/m^2 making it possible to increase the peel strength with higher binder grammages. The

FIGURE 15 Overview over damages observed after T-peel testing; lay-ups: (A) ±45°/±45° (80 g/m^2), (B) UD/UD (40 g/m^2), (C) (0°/90°)/(0°/90°) (80 g/m^2)

covered surface does roughly double when increasing the binder grammage from 20 to 80 g/m^2. The measured peel force however increases from 1.1 to 4.2 N/cm. It has to be considered that the textiles do not have a flat solid surface like the paper does. During joining of the layers the tows may deform depending on the compaction pressure used. The binder may flow into voids in between rovings increasing the covered surface. As the compaction pressure was not varied during the investigation, no final conclusion can be made here.

Comparing the measured peel forces with the measurements of Dickert[24] and Zhao[33] shows the spray binder reaches high peel forces compared to most powder binders or veils. For a binder grammage of 2 wt% (about equal to 20 g/m^2 in this paper) Dickert[24] measured peel strengths of 1.6 N/cm for one epoxy binder powder and below 0.5 N/cm for other epoxy, phenoxy and copolyamide binders. Both used textiles different from the ones used in this paper. Dickert used a biaxial carbon fiber non-crimped fabric with a grammage of 308 g/m^2 and a fiber orientation of ±45°. Zhao[33] found a peel strength of around 0.37 N/cm for a polyamide based binder system using a binder content of 2.5 wt% and a carbon fiber four-harness satin woven fabric with a grammage of 220 g/m^2. However, the differences between the measured values are still significant even when considering different textiles. This leads to the assumption that the form fixation of the spray binder is sufficient for preforming which is further supported by looking at the samples after the peel test: All textile layers were damaged. The damages found range from fiber pull-out to failure of the knitting yarn. An overview of the observed damages is shown in Figure 15. Since the samples for the T-peel test are only 25 mm wide, the fibers in 45° and 90° direction are short and only held together by the knitting yarn. This resulted in failure of the textile for higher binder grammages.

3.4 | Three-point flexural bending

The results of the three point flexural bending test are displayed in Figures 16 and 17. The unidirectional lay-ups have higher flexural modulus and stress than the biaxial lay-ups. This can be explained by the layer orientation in the different samples. The unidirectional fibers run in 0°-direction, the direction of force flow during the experiment. Thus, they are able to take part in force transmission. This also applies to the 0°-layer of the biaxial textile when cut into 0°/90°-samples. The 90°-layers lay perpendicular to the force flow and can easily be bent. They are only held together by the knitting yarn and binder. The same applies to the biaxial textile when cut into ±45° layers. Due to the width of the samples being only 25 mm the tows are cut into short tows, which also have the wrong orientation for optimal force transmission. The fibers are again only connected by knitting yarn and binder.

Compared to the binderfree lay-ups, the bindered textile have significantly higher flexural modulus and flexural stress. However, both values seem to reach an upper limit within the tested grammages. At 60 mm/min the maximum flexural stress is higher than at 4 mm/min for all lay-ups which is expected as the mechanical

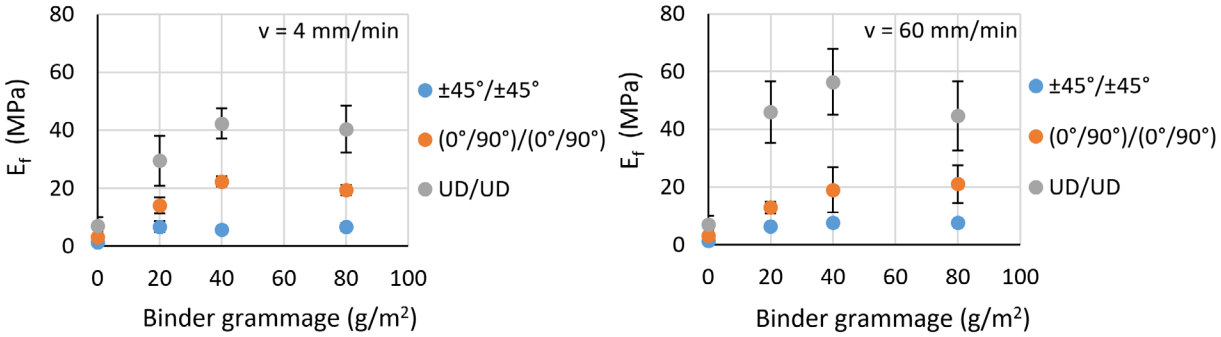

FIGURE 16 Flexural modulus for different lay-ups, binder grammages and test speeds

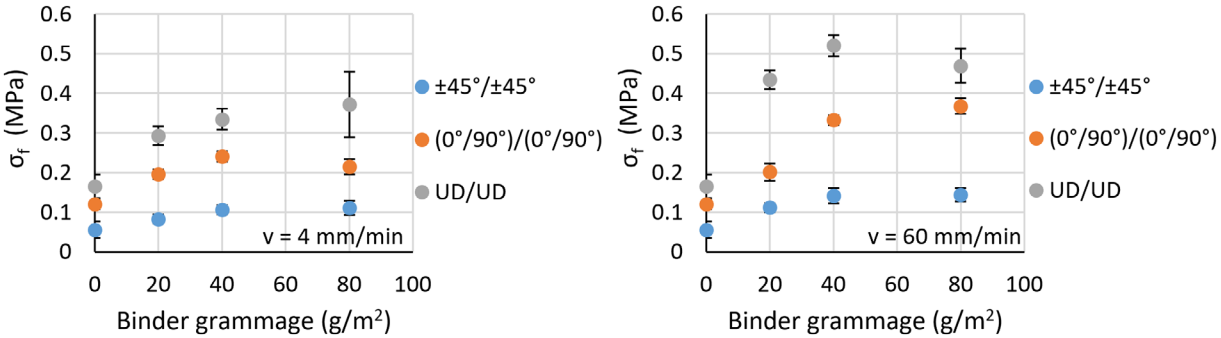

FIGURE 17 Maximum flexural stress for different lay-ups, binder grammages and test speeds

properties of polymers are depended on loading velocity. When comparing the flexural modulus, a noticeable increase was only observed for the unidirectional samples. The (0°/90°)-samples and the ±45° samples show almost no difference in flexural modulus.

Looking at values from literature, Dickert[24] made three point flexural tests with powder binders. He found a linear growth of flexural modulus and stress for rising binder grammage. Coutandin et al. [46] found a linear increase in flexural modulus for rising binder grammage, as well. This does not apply to the spray binder tested in this publication. A possible explanation for this difference can be found by looking at the state of the binders at room temperature, which is the temperature the samples were tested at. Powder binders and veils are solid at room temperature, resulting in a preform with increasing stiffness for higher binder grammages. The spray binder is still liquid at room temperature with high viscosity. While bending, the spray binder does not fail but can easily start creeping under load. After releasing the flexural force, the samples stay in their deformed shape but slowly return to their initial state. The measured flexural modulus is also lower than the ones found in Dickert[24] and Coutandin et al. [46] for powder binders, while the flexural stress reaches similar values when using a test speed of 60 mm/min. In both publications, the initial flexural modulus of the plain textile without binder is already higher (50 MPa for Dickert and 380 MPa for Coutandin et al.) making it difficult to directly compare the results. Coutandin also used a different test setup (cantilever beam test). The lower stiffness and the non-solid state at room temperature of AM1010 however, could lead to difficulties when trying to handle large and thick preforms outside of their original mold as the binder may start creeping under high loads or the preform might deform.

4 | CONCLUSION

Properties of preforms made with spray binder and their manufacturing process were investigated in this publication. For the manufacturing of bindered preforms, it is important to analyze the temperature-dependent properties of the binder used. The swirl spray pattern necessary to reach even binder application was only achieved within a small temperature window. Deviating from the optimal temperature window might lead to uneven binder application. Binder flow could be controlled by adjusting the material pressure in the spray system. Adjusting the material pressure during the process opens the possibility for varying binder grammages in different areas of the preform.

The spray binder used in this paper offers sufficient form fixation of the preform as shown by T-peel tests. The force needed to separate the layers is higher than for many powder binders or veils presented in literature. However, these differences might be influenced by the use of dissimilar textiles in different publications. To fully evaluate the difference between the different binder systems additional experiments with different binder systems while using the same textiles are needed. Further investigation also has to be done regarding the handling strength of preforms made with spray binders. The results of the three-point-flexural bending tests suggest lower flexural moduli than preforms made with powder binder. When removing preforms from the mold they are initially made in, the preforms might relax back into their original shape or the binder may start creeping under high load. This problem should be less of an issue when the infusion step is made in the same mold as the preforming for example in the manufacturing of rotor blades for wind turbines. In this case the mold can stabilize the preform while the binder prevents slipping of the layers for example on mold parts with high gradients. T-peel and three point flexural test results also showed the importance of comparing the textiles used when comparing test results for different binders. Depending on the general architecture of the textile, the fiber orientation and the surface area of the textiles the results can widely vary.

To fully understand the influence of spray binder on the whole LCM process chain, further tests regarding the influence of spray binder on the infusion step as well as the mechanical properties of the final part are necessary.

ACKNOWLEDGMENTS

The authors would like to thank the federal state of Lower Saxony and the European Regional Development Fund (ERDF) for financial and organizational support of the project AutoBLADE. The binder was supplied free of charge by CTP Advanced Materials. Open Access funding enabled and organized by Projekt DEAL.

DATA AVAILABILITY STATEMENT

The data that support the findings of this study are available from the corresponding author upon reasonable request.

ORCID

Hendrik Möllers https://orcid.org/0000-0002-4568-6339

REFERENCES

[1] C. Cherif, *Textile Werkstoffe für den Leichtbau*, Springer Berlin Heidelberg, Berlin, Heidelberg **2011**.

[2] M. Tonejc, Chancen und Herausforderungen bebinderter Textilien in der Faserkunststoffverbund-Verarbeitung. *Dissertation*, Leoben **2019**.

[3] M. Belhaj, M. Deleglise, S. Comas-Cardona, H. Demouveau, C. Binetruy, C. Duval, P. Figueiredo, *Compos. B: Eng.* **2013**, *50*, 107.

[4] S. Coutandin, *Prozessstrategien für das automatisierte Preforming von bebinderten textilen Halbzeugen mit einem segmentierten Werkzeugsystem*. *Dissertation*, Karlsruhe **2020**.

[5] L. Daelemans, S. van der Heijden, I. de Baere, I. Muhammad, W. van Paepegem, H. Rahier, K. de Clerck, *Compos. B: Eng.* **2015**, *80*, 145.

[6] O. Rimmel, D. Becker, P. Mitschang, *Adv. Manuf.: Polym. Compos. Sci.* **2016**, *2*, 93.

[7] P. Moll, S. Wang, S. Coutandin, J. Fleischer, *Text. Res. J.* **2020**, *91*, 664.

[8] J. C. Brody, J. W. Gillespie, *J. Thermoplast. Compos. Mater.* **2005**, *18*, 157.

[9] S. Schmidt, T. Mahrholz, A. Kühn, P. Wierach, *Polym. Compos.* **2018**, *39*, 708.

[10] S. Schmidt, T. Mahrholz, A. Kühn, P. Wierach, *J. Compos. Mater.* **2019**, *53*, 2261.

[11] U. Beier, J. K. Sandler, V. Altstädt, H. Spanner, C. Weimer, *Compos. Part A: Appl. Sci. Manuf.* **2009**, *40*, 1756.

[12] F. Helber, M. Szcesny, S. Carosella, P. Middendorf, in *ICCM 22*, **2019**.

[13] F. Helber, A. Amann, S. Carosella, P. Middendorf, *IOP Conf. Ser.: Mater. Sci. Eng.* **2018**, *406*, 12064.

[14] A. K. Kadiyala, A. Portela, K. Devlin, S. Lee, A. O'Carroll, D. Jones, A. Comer, *Compos. Sci. Technol.* **2021**, *201*, 108512.

[15] R. W. Hillermeier, J. C. Seferis, *Compos. Part A: Appl. Sci. Manuf.* **2001**, *32*, 721.

[16] R. Böhme, L. Girdauskaite, I. Jansen, S. Krzywinski, *Lightweight Des.* **2010**, *3*, 55.

[17] R. Braun, *Gemeinsamer technischer Schlussbericht zum Verbundprojekt BladeMaker*, Bremerhaven **2018**.

[18] J. Fleischer, F. Ballier, M. Dietrich, *Appl. Mech. Mater.* **2016**, *840*, 66.

[19] J. Franke, J.-H. Ohlendorf, K.-D. Thoben, *Materialwiss. Werkstofftech.* **2019**, *50*, 1326.

[20] L. Girdauskaite, S. Krzywinski, H. Rödel, A. Wildasin-Werner, R. Böhme, I. Jansen, *Appl. Compos. Mater.* **2010**, *17*, 597.

[21] J. C. Brody, J. W. Gillespie, *Polym. Compos.* **2005**, *26*, 377.

[22] M. Dickert, Einfluss von Binder auf die Herstellung von Faserkunststoffverbunden. *Dissertation*, Clausthal **2015**.

[23] M. Tanoğlu, A. T. Seyhan, *Mater. Sci. Eng.: A* **2003**, *363*, 335.

[24] G. Estrada, C. Vieux-Pernon, S. G. Advani, *J. Compos. Mater.* **2002**, *36*, 2297.

[25] D. Magagnato, B. Thoma, F. Henning, *Zeitschrift Kunststofftechnik* **2015**, *1*, 256.

[26] O. Rimmel, Grundlagen der Imprägnierung von Dry Fiber Placement Preforms. *Dissertation*, Kaiserslautern **2020**.

[27] M. Tonejc, C. Ebner, E. Fauster, R. Schledjewski, *Adv. Manuf.: Polym. Compos. Sci.* **2019**, *5*, 128.

[28] H. M. Yoo, J. W. Lee, J. S. Kim, M. K. Um, *Appl. Sci.* **2020**, *10*, 7039.

[29] M. Tanoglu, S. Robert, D. Heider, S. H. McKnight, V. Brachos, J. W. Gillespie, *Int. J. Adhes. Adhes.* **2001**, *21*, 187.

[30] M. Tanoğlu, A. T. Seyhan, *Int. J. Adhes. Adhes.* **2003**, *23*, 1.

[31] X. Zhao, W. Chen, X. Han, Y. Zhao, S. Du, *Compos. Sci. Technol.* **2020**, *191*, 108094.

[32] S. Dutta, M. Körber, C. Frommel, *Procedia CIRP* **2019**, *85*, 329.

[33] J. Mack, Entwicklung eines adaptiven Online-Bebinderungsprozesses für die Preformherstellung. *Dissertation*, Kaiserslautern **2015**.

[34] O. Rimmel, J. Mack, D. Becker, P. Mitschang, *Lightweight Des. Worldw.* **2017**, *10*, 48.

[35] P. Cognard, *Adhesives and Sealants - General Knowledge, Application Techniques, New Curing Techniques*, Elsevier, Versailles, **2006**, 51-xxxvii.

[36] S. Horiashchenko, K. Horiashchenko, J. Musial, *Mechanika* **2020**, *26*, 82.

[37] B. Denkena, C. Schmidt, S. Werner, D. Schwittay, *J. Compos. Sci.* **2021**, *5*, 93.

[38] DIN Deutsches Institut für Normung, *Klebstoffe – T-Schälprüfung für geklebte Verbindungen aus flexiblen Fügeteilen, 83.180*, Beuth Verlag, Berlin **2010**.

[39] DIN Deutsches Institut für Normung, *Faserverstärkte Kunststoffe – Bestimmung der Biegeeigenschaften, 83.120*, Beuth Verlag, Berlin **2011**.

[40] J. Hepperle, in *Co-Rotating Twin-Screw Extruder* (Ed: K. Kohlgrüber), Carl Hanser Verlag GmbH & Co. KG, München **2007**, p. 35.

[41] F. Mustata, I. Bicu, *J. Appl. Polym. Sci.* **2000**, *77*, 2430.

[42] N. Vernet, E. Ruiz, S. Advani, J. B. Alms, M. Aubert, M. Barburski, B. Barari, J. M. Beraud, D. C. Berg, N. Correia, M. Danzi, T. Delavière, M. Dickert, C. Di Fratta, A. Endruweit, P. Ermanni, G. Francucci, J. A. Garcia, A. George, C. Hahn, F. Klunker, S. V. Lomov, A. Long, B. Louis, J. Maldonado, R. Meier, V. Michaud, H. Perrin, K. Pillai, E. Rodriguez, F. Trochu, S. Verheyden, M. Wietgrefe, W. Xiong, S. Zaremba, G. Ziegmann, *Compos. Part A: Appl. Sci. Manuf.* **2014**, *61*, 172.

[43] CTP Advanced Materials GmbH, *TDS CeTePox AM 1010: Preliminary Technical Data Sheet*, 2020.

[44] V. T. Marla, R. L. Shambaugh, D. V. Papavassiliou, *Ind. Eng. Chem. Res.* **2006**, *45*, 2331.

[45] I. Formoso, A. Rivas, G. Beltrame, G. S. Larraona, J. C. Ramos, R. Antón, A. Salterain, *J. Ind. Text.* **2020**, *51*(3), 152808372097840.

[46] S. Coutandin, A. Wurba, A. Luft, F. Schmidt, M. Dackweiler, J. Fleischer, *Materialwiss. Werkstofftech.* **2019**, *50*, 1573.

How to cite this article: H. Möllers, C. Schmidt, D. Meiners, *Polym. Compos.* **2023**, *44*(1), 432. https://doi.org/10.1002/pc.27107